XL CILAMCE
IBERO-LATIN AMERICAN CONGRESS ON COMPUTATIONAL METHODS IN ENGINEERING
NOVEMBER 11-14, 2019
Praiamar Natal Hotel & Convention Natal, RN-BRAZIL

DISTORTIONAL STRENGTH OF COLD-FORMED STEEL PINNED-FIXED LIPPED CHANEL COLUMNS

Warlley S. Santos
warlley.santos@vale.com
VALE – Unidade de Tubarão
Av. Dante Michelini, 5500 Ponta de Tubarão, Ed. Israel David Rosenberg, 29090-900 Vitória ES, Brasil
Alexandre Landesmann
alandes@coc.ufrj.br
PEC/COPPE - Instituto Alberto Luiz Coimbra, Universidade Federal do Rio de Janeiro
Rua Horácio Macedo, Bloco i, sl 216 (Centro de Tecnologia), 21941-450 Rio de Janeiro, Brasil
Dinar Camotim
dcamotim@civil.ist.utl.pt
CERIS, Instituto Superior Técnico, Universidade de Lisboa, Av. Rovisco Pais 1, 1049-001 Lisboa, Portugal

Abstract.

This work addresses the buckling behaviour, ultimate strength and Direct Strength Method (DSM) design of pinned-fixed (bolted-fixed) cold-formed steel lipped channel columns, selected to fail in distortional modes. The end-connections consist of a pair of cylindrical high-strength bolts with hexagonal head and nut, which are inserted in two standard-size holes located at the intersections of the flanges with the principal centroidal axis parallel to the web – on the other hand, the fixed end support consist a welded end-plate. After selecting the columns with various combinations of geometry (length and cross-section dimensions) and yield stresses, Ansys Shell Finite Element (SFE) analyses are used to investigate the failure modes of selected columns and assemble ultimate strength data. Together with experimental failure data previously reported by authors out at the Federal University of Rio de Janeiro, these values are then employed (i) to assess the merits of the current DSM design curves and, in view of their inadequacy, (ii) to propose new strength curves that provide efficient failure load predictions for the whole set of columns considered.

Keywords: Cold-formed steel lipped channel columns; Bolted and fixed end support conditions; Distortional failure.

1 Introduction

Cold-formed steel profiles are widely used in the construction industry since they provide high structural efficiency (large strength-to-weight ratio), low production and erection costs and notable fabrication versatility. Many cold-formed steel members are prone to distortional failure, the current design specifications include provisions dealing with this collapse mode. In particular, the Direct Strength Method (DSM – *e.g.*, [1]), prescribed by the current North-American Specification for the Design of Cold-Formed Steel Structural Members (AISI 2016 [2]), contains specific provisions, namely strength curves, for the design of columns and beams against distortional collapses. Generally, compressive thin-walled column tests are conducted on rigid plates welded in the specimen's end cross-sections (*e.g.* [3-5]). Furthermore, the existing DSM expressions were calibrated against experimental results concerning mostly fixed columns (rigid plates attached to their end sections) [6]. Even though a

considerable number of researches reported in the literature that studied cold-formed columns with fixed ends, building construction industries have used bolted connections for structural assemblies. At this stage, it is worth mentioning a previous numerical investigation carried out by the authors [7] on the distortional failure strength of simply-supported (end sections locally/globally pinned and allowed to warp freely) cold-formed steel columns with several cross-section shapes, which provided solid evidence that the current DSM design curve [2] is unable to predict adequately (safely and accurately) the failure loads of such columns – indeed, it was found that this design curve overestimates the failure load of most cold-formed steel columns, namely the lipped channel ones. The main objective of this work is to report the results of a numerical investigation concerning the influence of one pinned-fixed end support conditions on the failure and DSM-based design of cold-formed steel lipped channel

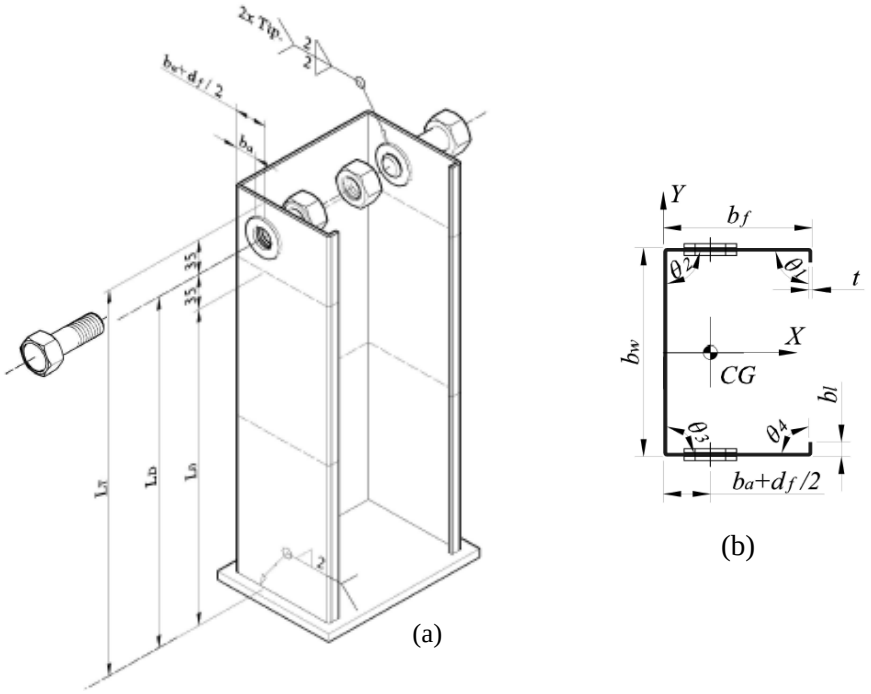

columns buckling and failing in distortional modes, which was initiated by Santos [8].

Figure 1. Pinned-fixed lipped channel columns: (a) overall view and (b) cross-section dimensions

2 Column Geometry Selection

The first task of this work consisted of selecting the pinned-fixed (bolted-fixed) lipped channel columns to be analyzed numerically, which are supposed to (i) exhibit cross-section dimensions commonly used in practice, with various wall width proportions (mostly web-to-flange width ratios), (ii) buckle and fail in distortional modes, and (iii) have lengths associated with single half-wave critical buckling modes. The selection procedure was performed by means of ANSYS [9] shell finite element buckling analyses. Fortunately, it was possible to fulfil the requirements listed before and the selection procedure led to the *15* lipped channel column cross-section dimensions and lengths (L_D) given in Table 1 – see also Figure 1(b). Note that the selected columns consist of five triplets, each of them sharing the same web width and with web-to-flange width ratios (b_w/b_f) equal to $\approx$*0.7, 1.0* and $\approx$*1.43* – the column labels consist of the $b_w \times bf$ widths (both in mm), while t*=2.65 mm* and b_l*=10.5 mm* are the same for all the columns. Table 1 also provides the column (i) nominal cross-section areas *A*, (ii) web-to-flange width ratios b_w/b_f, (iii) critical distortional buckling loads P_{crD}, calculated with *E=205 GPa* and *v=0.3* (steel Young's modulus and Poisson's ratio) and (iv) bifurcation-to-critical buckling load ratios $P_{b1.L}/P_{crD}$ and $P_{b1.G}/P_{crD}$, where $P_{b1.L}$ and $P_{b1.G}$ are the lowest local and global bifurcation loads – these ratios lie inside the intervals *1.35-2.16* and *13.1-133*. For illustrative purposes, Figure 2 shows the 100×70 column signature curve, providing the variation of its critical buckling load P_{cr} with the length L (logarithmic scale) – also shown are the selected column length L_D and critical (distortional) buckling mode shape.

Table 1. Selected lipped channel column cross-section dimensions, lengths, critical loads and bifurcation-to-critical load ratios

Column ($b_w \times b_f$)	b_w (*mm*)	b_f (*mm*)	$\frac{b_w}{b_f}$	A (cm^2)	L_D (*mm*)	P_{crD} (*kN*)	$\frac{P_{b1.L}}{P_{crD}}$	$\frac{P_{b1.G}}{P_{crD}}$
100×70		70	1.43	6.52	400	349	1.35	13.1
100×100	100	100	1.00	8.11	450	234	1.64	15.5
100×142.9		142.9	0.70	10.38	600	154	1.66	20.0
130×91		91	1.43	8.43	450	264	1.41	22.1
130×130	130	130	1.00	10.5	550	171	1.66	30.2
130×185.7		185.7	0.70	13.45	650	113	1.97	41.9
150×105		105	1.43	9.7	500	214	1.44	33.4
150×150	150	159	1.00	12.09	650	145	1.68	45.5
150×214.3		214.3	0.70	15.49	750	96.4	1.76	64.8
180×126		126	1.43	11.61	600	175	1.49	57.5
180×180	180	180	1.00	14.47	700	119	1.73	80.8
180×257.1		257.1	0.70	18.56	900	77.3	2.14	106
200×140		140	1.43	12.88	600	154	1.52	74.7
200×200	200	200	1.00	18.06	750	103	1.72	96.5
200×285.7		285.7	0.70	20.6	950	67.0	2.16	133

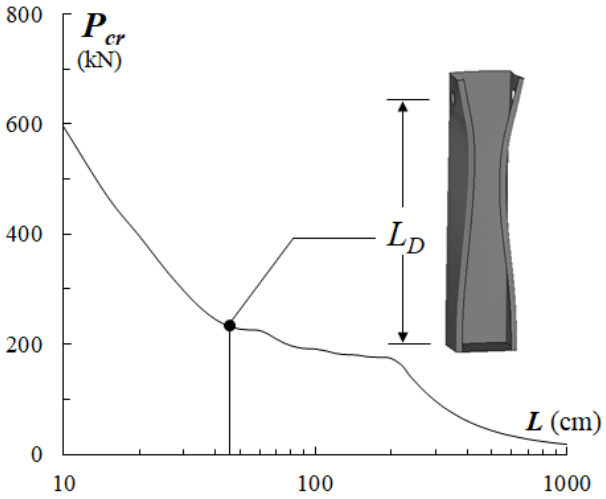

Figure 2. 100×70 column signature curve and selected column length and distortional buckling .

3 Ansys Shell Finite Element Model

The column linear buckling and geometrically non-linear elastic-plastic analyses were carried out in code Ansys [9], employing shell finite element model involving column discretization into fine Shell181 element meshes – 4-node shear deformable thin-shell elements with six degrees of freedom per node and full integration. Convergence studies [8] showed that accurate results can be obtained, with a reasonable computational effort, by (i) discretizing the member into a 5×5 *mm* mesh and (ii) refining this mesh in the close vicinity of the rounded corners and, mostly, around the bolt holes – Figure 3(a) shows a general view of the Shell Finite Element (SFE) mesh adopted to perform the column analyses in this work. An estimation of the circular arc angle/length along which the contact between the bolt and the hole surface takes place – a value of $97°$ was found [8] (see the zoomed view at the right of Figure 3(b)) and the two bolt hole arc surfaces ensuring each end support condition – see right side of Figure 3(b). Assume that, in each bolt, the compressive load is applied through radial surface stresses linearly

distributed along the *97°* contact circular arc length, as depicted in the left side of Figure 13(b) – in each bolt [9-10, 12-14], the transversal and longitudinal resultants of these radial surface stresses are null and equal to half of the applied compressive load, respectively. The value of the above radial surface stress linear distribution is determined by means of analytical expressions written in the first author's Ph.D. thesis [8]. Concerning the bolted support conditions, the SFE model considers simple supports along the two bolt *97°* contact circular arc lengths, as illustrated on the right side of Figure 3(b). These supports prevent the hole surface displacements normal to the web surface, while keeping their in-plane and longitudinal counterparts free. Moreover, to preclude column rigid body motions, the *97°* contact circular arc length mid-point in-plane and mid-span mid-web axial displacements were prevented (note that the loading consists of equal compressive forces applied at the two end bolt pairs). The boundary conditions adopted on the fixed end plate (*8 mm* thick) was restricted over all directions and rotations.

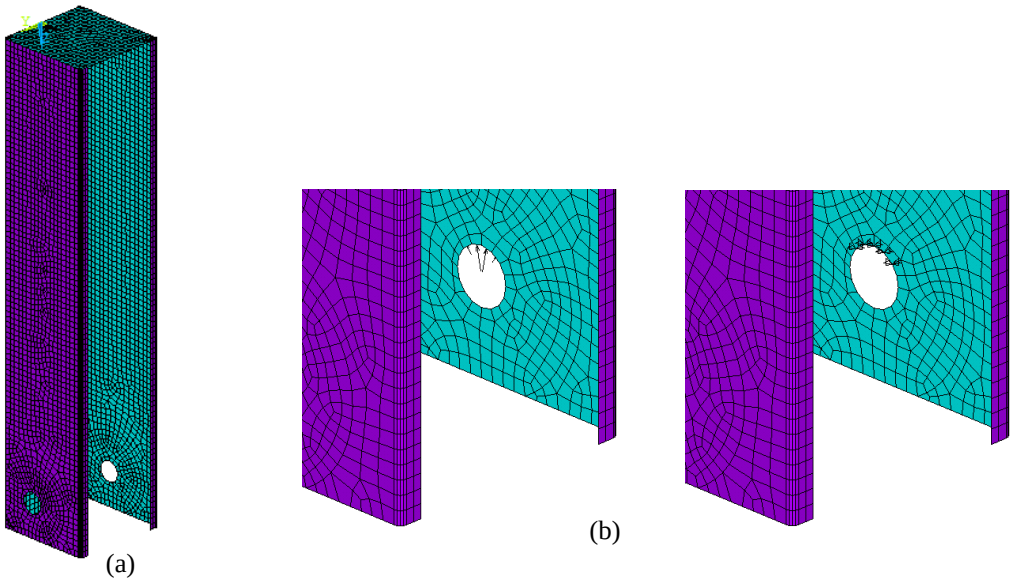

Figure 3. Column SFE discretization: (a) general view and (b) loading and support conditions concerning the SFE model

The geometrically and materially non-linear Ansys SFE analyses carried out to determine the column failure loads were performed by means of an incremental-iterative technique that combines Newton-Raphson's method with an arc-length control strategy – the applied compressive forces are increased in small increments, taking advantage of the Ansys automatic load stepping procedure. All the columns analyzed (i) contain critical-mode (distortional) initial geometrical imperfections with small amplitudes (maximum equal to *19%* of the wall thickness *t*, which corresponds to the average of the values measured in the specimens tested), and (ii) exhibit an elastic-perfectly plastic material behavior (Prandtl-Reuss model: von Mises yield criterion and associated flow rule), characterized by $E=205\ GPa$, $\nu=0.3$ and several yield stresses f_y. No strain-hardening, residual stresses (not measured in the tested specimens) and/or corner strength effects were included in the analyses – it has been reported in the literature (*e.g.*, [10]) that the combined influence of strain hardening, residual stresses and rounded corner effects has little impact on the column failure load.

The incorporation of the critical-mode initial geometrical imperfections is made automatically by (i) determining the column critical buckling mode shape, through an Ansys SFE linear buckling analysis (adopting the same discretization employed to carry out the subsequent non-linear analysis), (ii) scaling it to exhibit a maximum displacement equal to $0.19\ t$ and (iii) "transforming" this buckling output into an input of the non-linear analysis.

3.1 Parametric Study – Numerical Failure Loads

The aim of this section is to present the numerical failure load data gathered from the parametric study carried out, involving a total of *210* columns, which corresponds to all possible combinations of the (i) *15* column geometries given in Table 1 and (ii) *14* yield stresses (f_y) considered, selected to enable covering a quite wide distortional slenderness (λ_D) range, varying between *0.4* and *3.5* – recall that $\lambda_D=(P_y/P_{cr.D})^{0.5}$, where $P_y=A\cdot f_y$ is the squash load (A is the cross-section area, given in Table 1). Tables in the first author's Ph.D. thesis [8] provide information concerning the column numerical failure loads.

Figure 4(a) plots the numerical failure load ratio P_u/P_y against λ_D for all the columns analyzed in this work. One readily notices a huge P_u/P_y vertical dispersion in the low and moderate slenderness ranges (λ_D below around *1.75*). In order to identify the source of this very surprising finding, the numerical failure loads of the columns involved were inspected in detail. This inspection revealed that *72* stocky columns (all with f_y below *387 MPa*) collapse prematurely, due to the occurrence of localized yielding in the flange regions located below the flat washers (see Figures 1 and 3(b)) and, therefore, never exhibit significant distortional deformations – all the remaining columns fail in clear distortional modes. This is illustrated in Figures 5(a)-(b), which display the failure modes and von Mises stress (σ_{VM}) contours of 100×100 columns with slenderness $\lambda_D=0.86$ and $\lambda_D=1.31$, respectively – the distinct failure mode natures are clearly visible: while the first column fails by localized yielding where it is not possible to see high tensions at ¼-height cross-section (near the holes) on edge stiffeners, the collapse of the second one is purely distortional in which it is verified by deformation and high tensions at ¼-height cross-section (also near the holes) on edge stiffeners. Figure 4(b) shows the P_u/P_y *vs.* λ_D plot when all the columns failing by localized yielding are excluded – it is readily observed that the P_u/P_y "cloud" is fairly well aligned along a "Winter-type" strength curve, with very little vertical dispersion.

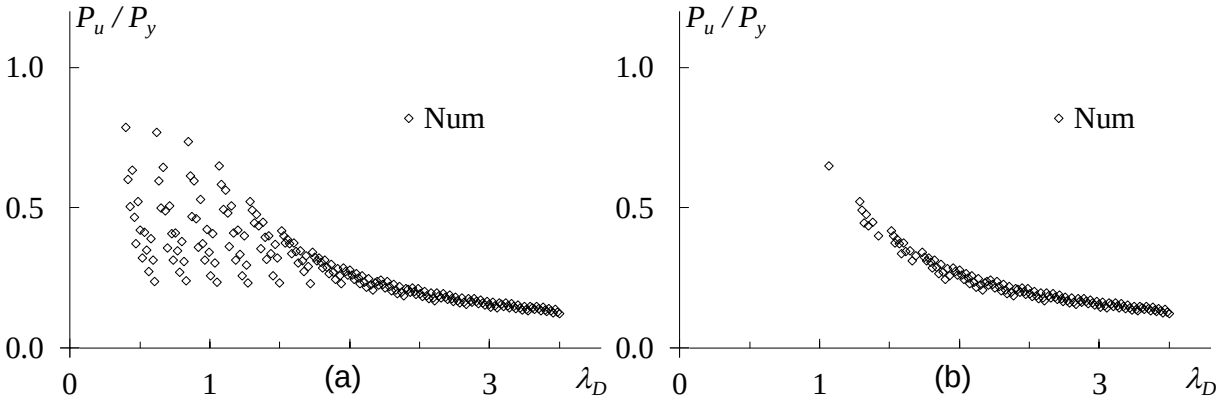

Figure 4. Plots P_u/P_y *vs.* λ_D concerning (a) all the original columns and (b) all the original columns failing in distortional modes

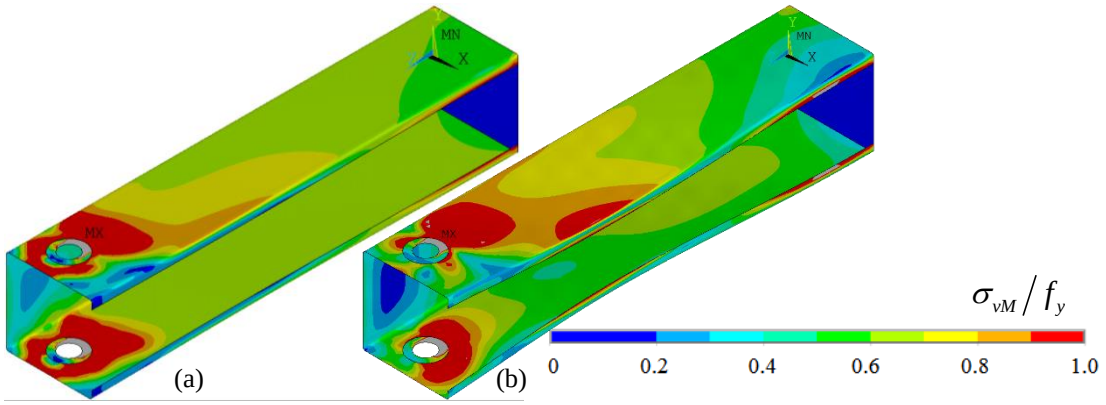

Figure 5. Collapse modes and von Mises stress contour of 100x100 columns: (a) localized ($\lambda_D=0.86$) and (b) distortional ($\lambda_D=1.31$) failure

4 DSM Design Considerations

Attention is now turned to assessing the performance of the available DSM columns distortional strength curves in predicting of the failure loads of the end-bolted lipped channel columns numerically analyzed in this work. In particular, the currently codified design curve [2], which provides failure load estimates (P_{nD}) given by

$$\frac{P_{nD}}{P_y} = \begin{cases} 1 & \text{for } \lambda_D \le 0.561 \\ \left[1 - 0.25\left(\lambda_D^{-1.2}\right)\right]\left(\lambda_D^{-1.2}\right) & \text{for } \lambda_D > 0.561 \end{cases} \tag{1}$$

Figure 6(a) compares this design curve with the (i) numerical (white lozenges) and (ii) experimental (crosses) failure load ratios P_u/P_y [8]. Moreover, Figure 6(b) plots, also against λ_D, the "exact"-to-predicted failure load ratios P_u/P_{nD}, providing a pictorial representation of the failure load estimation quality achieved by the current design curve – also indicated are the P_u/P_{nD} statistical indicators (averages, standard deviations and maximum/minimum values of the numerical and experimental results) – concerning (i) the 10 specimens experimentally tested [8] and (ii) the complete set of columns numerically analyzed in this parametric study. The observation of these results prompts the following remarks:

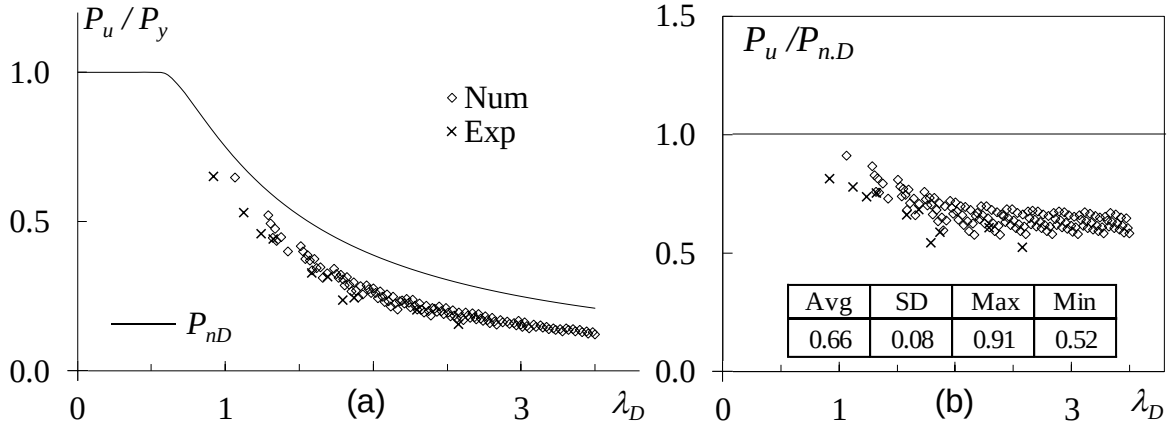

Figure 6. (a) Comparison of the current DSM distortional design curve P_{nD} with the column failure load ratios P_u/P_y, and (b) associated failure-to-predicted load ratios plot against λ_D

(i) It is readily noticed that the numerical and experimental failure loads are grossly overestimated by the current DSM design curve, as quantified by the corresponding P_u/P_{nD} statistical indicators, which read *0.66-0.08-0.91-0.52* – note that the amount of overestimation increases with λ_D. It is worth recalling that the calibration and validation of this DSM design curve was based almost exclusively on failure loads of columns with rigid plates attached to their end cross-sections, thus fully preventing their warping [1].

(ii) Findings similar to those described in the previous item were reported in [7], on the basis of numerical failure loads of standard simply supported columns. It was concluded that the significant differences in distortional post-critical strength, stemming from the end cross-section warping restraint (warping fully prevented or completely free), are not adequately reflected by the distortional critical buckling stresses. Based on the numerical failure loads gathered, the authors preliminarily proposed an alternative DSM design curve for simply supported columns, which provides failure load estimates ($P_{nD.SS}$) given by

$$\frac{P_{nD.SS}}{P_y} = \begin{cases} 1 & \text{for } \lambda_D \le 0.561 \\ \left[1 - 0.25\left(\lambda_D^{-1.2}\right)\right]\left(\lambda_D^{-1.2}\right) & \text{for } 0.561 < \lambda_D \le 1.133 \\ \left[0.65 + 0.2\left(\lambda_D^{-1.5}\right)\right]\left(\lambda_D^{-1.5}\right) & \text{for } \lambda_D > 1.133 \end{cases} \tag{2}$$

only differing from the currently codified ones (see Eq. (1)) for $\lambda_D > 1.133$. Figure 7(a) makes it possible to compare this proposed design curve (red line) with the failure load ratios P_u/P_y considered in this work – the corresponding $P_u/P_{nD.SS}$ values are plotted against λ_D in Figure 7(b). These plots clearly show the failure load prediction quality improvement achieved by the strength curve proposed in [7], spanning the whole distortional slenderness range, as attested by the $P_u/P_{nD.SS}$ indicators: *1.08-0.12-1.32-0.77*.

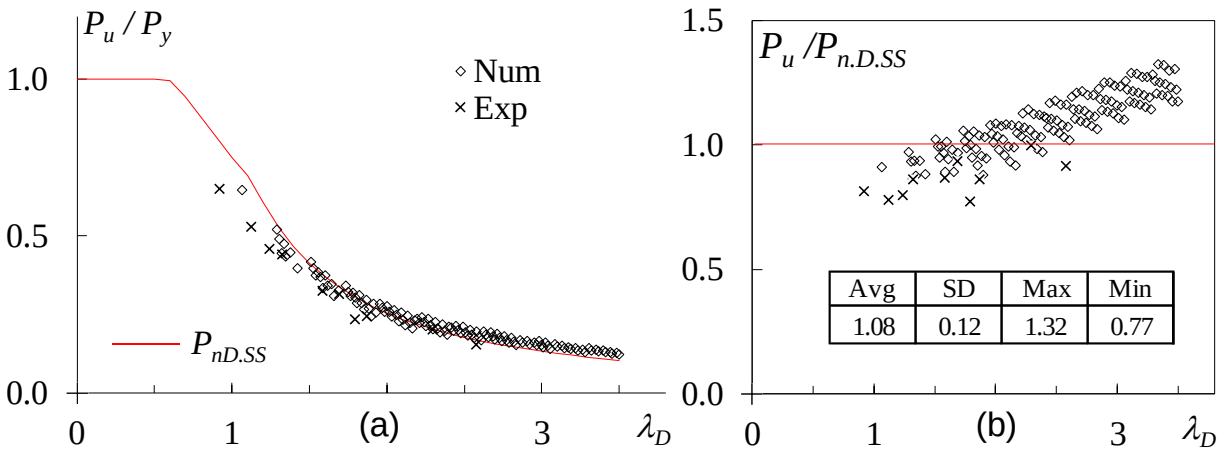

Figure 7. (a) Comparison of the DSM distortional design curve proposed in **[7]** ($P_{nD.SS}$) with the column failure load ratios P_u/P_y and (b) associated failure-to-predicted load ratios plot against λ_D

4.1 Modification of the Proposed DSM-Based Design Curve

On the basis of the experimental and numerical failure load data obtained in this work, a first attempt is made here to find a modified DSM-based design curve capable of providing adequate (safe, accurate and reliable) predictions for the failure loads of the pinned-fixed columns considered in this work and collapsing in distortional modes. Adopting the approach employed previously in [7], the authors carried out a "trial-and-error" curve fitting procedure – its output, denoted $P_{nD.EB}$, is the modified/lowered DSM-based strength curve

$$\frac{P_{nD.EB}}{P_y} = \begin{cases} \left(0.620^{\lambda_D^{1.85}}\right) & \text{for } \lambda_D \leq 1.588 \\ \left[0.55 + 0.2\left(\lambda_D^{-1.5}\right)\right]\left(\lambda_D^{-1.5}\right) & \text{for } \lambda_D > 1.588 \end{cases} \tag{2}$$

differing from the previous ones (Eqs. (1)-(2)) in the fact that (i) the flat yield plateau and initial portion of the descending curve (low and moderate slenderness ranges - λ_D below around *1.5*) are replaced by a single curve cast in the form of Johnson's parabola, (ii) the distortional slenderness transition value becomes *1.588* and (iii) the coefficient *0.65*, appearing in Eq. (2), is replaced by *0.55*. Figure 8(a) displays the $P_{nD.EB}$ strength curve (blue line) and the $P_u/P_{nD.EB}$ values are plotted against λ_D in Figure 8(b). It is readily observed that the failure load prediction quality improves quite significantly, as attested by the $P_u/P_{nD.EB}$ indicators: *1.26-0.15-1.55-0.90*. Moreover, note also that the number of unsafe failure load predictions falls considerably.

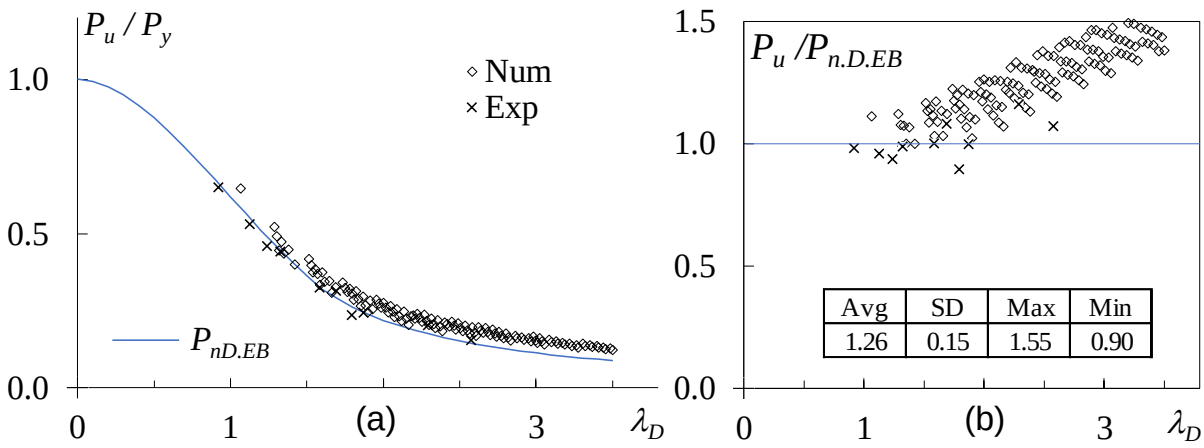

Figure 8. (a) Comparison of the modified/lowered DSM distortional design curve $P_{nD.EB}$ with the column failure load ratios P_u/P_y, and (b) associated failure-to-predicted load ratios plot against λ_D

5 Concluding Remarks

This work reported the results of an ongoing experimental and numerical investigation on the buckling, post-buckling and ultimate strength behaviour of lipped channel cold-formed steel pinned-fixed columns failing in distortional modes, which was initiated by Santos [8]. The numerical failure loads dealt in in this paper involved *15* lipped channel pinned-fixed (bolted) columns that were carefully selected (i) to ensure, as much as possible, "pure" distortional buckling and failure modes and (ii) to cover a wide (distortional) slenderness range. These results together with experimental ones originally reported by by Santos [8] were then used to assess the merits of the available DSM column distortional design curves in predicting them. It was found that the numerical and experimental ones reported by Santos [8] are overestimated by both (i) the currently codified design curve (all of them) and (ii) the strength curve proposed by Landesmann & Camotim [7] for standard simply supported columns. This finding led to the search for new DSM-based design approaches providing better quality failure load predictions for the pinned-fixed columns dealt with in this work. Further work is currently under way on this topic – it will be reported in the near future.

Acknowledgements

The first author gratefully acknowledges the financial support of Vale S.A. The second author gratefully acknowledge the financial support of the Brazilian institutions: CAPES (*Coordenação de Aperfeiçoamento de Pessoal de Nível Superior* - Finance Code 001), CNPq (*Conselho Nacional de Desenvolvimento Científico e Tecnológico*, 303860/2016-2) and FAPERJ (*Fundação Carlos Chagas Filho de Amparo à Pesquisa do Estado do Rio de Janeiro*, E-26/202.758/2017).

References

[1] B. W. Schafer, "Review: The Direct Strength Method of cold-formed steel member design," *Journal of Constructional Steel Research,* vol. 64, p. 766–778, 18 January 2008.

[2] AISI-S100, Specification for the design of cold-formed steel structural members, Washington, D. C.: American Iron and Steel Institute, 2016.

[3] B. Young, D. Camotim and N. Silvestre, "Ultimate strength and design of lipped channel columns experiencing local-distortional mode interaction - part I: Experimental Investigation," in *Proceedings of Sixth International Conference on Advances in Steel Structures*, Hong Kong, 2009.

[4] D. Yang and G. J. Hancock, Compression Tests of Cold-Reduced High Strength Steel Channel Columns failing in the Distortional Mode Research Report No R825, Sydney: Department of Civil Engineering - The University of Sydney, 2003.

[5] C. D. Moen and B. W. Schafer, "Experiments on cold-formed steel columns with holes," *Thin-Walled Structures,* vol. 46, p. 1164–1182, 14 March 2008.

[6] N. Silvestre, P. B. Dinis, D. Camotim and E. M. Batista, "DSM design of lipped channel columns undergoing local/distortional/global mode interaction," *SDSS'Rio 2010 Stability and Ductility of Steel Structures,* pp. 1061-1068, 8 September 2010.

[7] A. Landesmann and D. Camotim, "On the Direct Strength (DSM) design of cold-formed steel columns against distortional failure," *Thin-Walled Structures,* vol. 67, pp. 168-187, January 22 2013.

[8] W. S. Santos, On the Strength and DSM Design of End-Bolted Cold-Formed Steel Columns Buckling in Distortional Modes, Rio de Janeiro: PhD Thesis in Structural Engineering, COPPE, Federal University of Rio de Janeiro, 2017.

[9] Swanson Analysis System Inc., (SAS) Ansys Reference Manual (Vrs. 12), 2009.

[10] B. W. Schafer and T. Peköz, "Computational modeling of cold-formed steel characterizing geometric imperfections and residual stresses," *Journal of Constructional Steel Research,* pp. 193-210, 6 January 1998.